Article

Journal of
Nanoscience and Nanotechnology
Vol. 16, 12967–12970, 2016
www.aspbs.com/jnn

Copyright © 2016 American Scientific Publishers
All rights reserved
Printed in the United States of America

Optical Characteristics of Single-Crystal InGaN Nanowires Grown via Metal-Organic Chemical Vapor Deposition with a Ni Catalyst

Soon-Yong Kwon[1], Seul-Ki Moon[1], Chi Won Lee[1], Mohamed Ebaid[2, 3], Jin-Ho Kang[2], Sang-Wan Ryu[2], and Jin-Kyu Yang[1, *]

[1] *Department of Optical Engineering, Kongju National University, Cheonan 330-717, South Korea*
[2] *Department of Physics, Chonnam National University, Gwangju 500-757, South Korea*
[3] *Department of Physics, Faculty of Science, Beni Suef University, 62111 Beni Suef, Egypt*

High-density InGaN nanowires (NWs) were synthesized via metal-organic chemical vapor deposition on *r*-plane sapphire substrates at 720 and 730 °C. Scanning electron microscopy analysis indicated that the InGaN NWs grown at 720 °C were formed by the vapor-liquid-solid (VLS) process. However, the NWs grown at 730 °C were formed by sequential VLS and vapor-solid-solid processes. The optical properties of the single-crystal InGaN NWs were studied via micro-photoluminescence (μ-PL) and time-resolved μ-PL measurements under the excitation of a 403-nm laser diode. The internal quantum efficiency (IQE) of the NWs grown at 720 °C was approximately 100% below 150 K, which rapidly decreased to 58% at 300 K. However, the IQE of the NWs grown at 730 °C was approximately 100% below 100 K. The PL decay times of the NWs grown at 720 °C were less than those of the NWs grown at 730 °C over a temperature range of 8–300 K.

Keywords: Nanowire, Photoluminescence, InGaN.

1. INTRODUCTION

The importance of InGaN ternary alloys stems from the tunable band-gap emission of single-crystal InGaN, which spans the ultraviolet (UV) to infrared (IR) regions by simply adjusting the alloy composition.[1] This property of InGaN alloys combined with their stability under harsh experimental conditions has led to their use in many practical applications, including light-emitting diodes, laser diodes, solar cells, and solar-powered hydrogen generators that employ photoelectrochemical water splitting.[2] Reducing the dimensions of InGaN alloys to the nanoscale may also provide additional merits, e.g., increasing the In content and decreasing the strain in the alloy.[3] Furthermore, the interface between InGaN nanowires (NWs) and the substrate can effectively reduce the density of threading dislocations, and thus, increase the radiative efficiency by decreasing the number of non-radiative recombination centers.[4]

Recently, InGaN NWs have been synthesized via metal-organic chemical vapor deposition (MOCVD),[5] hydride vapor-phase epitaxy (HVPE),[6] and radio-frequency molecular-beam epitaxy (RF-MBE).[7, 8] However, the growth of InGaN NWs through HVPE is limited by H-induced In etching, which can significantly reduce the In content and form unreactive In species.[6] Even though the InGaN NWs grown by RF-MBE have a higher In content because of the reduced growth temperature, the high costs, slow growth rate, ultra-high vacuum requirements, and surface damage caused by the RF plasma source make the commercialization and practical application of this technique very difficult. On the other hand, MOCVD is known for its scalability in the growth of high-quality, single-crystal, III-V NWs that have sufficient In content to emit in the yellow-green spectrum.[5] Therefore, MOCVD is a promising technique for the growth of InGaN NWs.

In this study, InGaN NWs were grown via MOCVD at two different growth temperatures. The optical characteristics of the single-crystal InGaN NWs were analyzed

*Author to whom correspondence should be addressed.

at different temperatures by measuring their micro-photoluminescence (μ-PL) under continuous-wave (CW) excitation and time-resolved μ-PL (μ-TRPL) under ps-pulse excitation.

2. EXPERIMENTAL DETAILS

High-density InGaN NWs were synthesized via MOCVD on *r*-plane sapphire substrates by employing a Ni-initiated vapor-liquid-solid (VLS) growth technique. A 0.5-nm-thick Ni film was first deposited on a bare *r*-plane sapphire substrate with an electron-beam evaporator. The substrate was then loaded into the MOCVD reactor, where it was annealed at 900 °C for 10 min in a H atmosphere (100 Torr) to form nanoscale Ni catalysts. Immediately after the formation of the Ni catalysts, the reactor temperature was reduced to 720 °C and ammonia (NH_3), trimethylgallium (TMGa), and trimethylindium (TMIn) were introduced to the substrate as the N, Ga, and In precursors, respectively. The reactor pressure was maintained at 100 Torr during the 40 min growth cycle. To investigate the effect of the growth temperature on the optical properties of the InGaN NWs, another sample was prepared at 730 °C.

The optical properties of the single-crystal InGaN NWs were investigated via μ-PL and μ-TRPL spectroscopies. The μ-PL measurements were performed at different temperatures under the CW excitation provided by a 403-nm laser diode. The samples were placed inside a vibration-isolated closed-cycle cryostat and mounted on a nanopositioning stage with a minimum motor step of 10 nm at 8 K. The excitation beam was focused on a 1.7-μm-diameter area of the sample via a $\times$20-magnification, near-UV (NUV), objective lens (numerical aperture = 0.4, working distance = 17 mm). To obtain a PL spectrum, the emission light was collected onto the entrance slit of the spectrometer by the same objective lens. To investigate the recombination dynamics of the InGaN NWs, the decay time of the μ-PL was measured at different temperatures under the pulsed excitation provided by a 403-nm laser diode (pulse widths < 40 ps).

3. RESULTS AND DISCUSSION

Figure 1 shows the SEM images of the InGaN NWs grown at 720 and 730 °C. The InGaN NWs grown at 720 °C were formed by the VLS process, which is confirmed by the accumulation of metal particles at the tips of the obtained NWs (inset of Fig. 1(a)). In addition, because of the variation in the size of the Ni catalysts, the resulting NWs range from 300 nm to 3 μm in length, and from 100 to 350 nm in diameter. Figure 1(a) shows that the InGaN NWs have vertically aligned triangular cross sections, which correspond to the *c*-plane for the base and the [1$\bar{1}$01] plane for the two other facets.[9] On the other hand, increasing the growth temperature to 730 °C results in a decreased density of larger InGaN NWs. The inset of Figure 1(b)

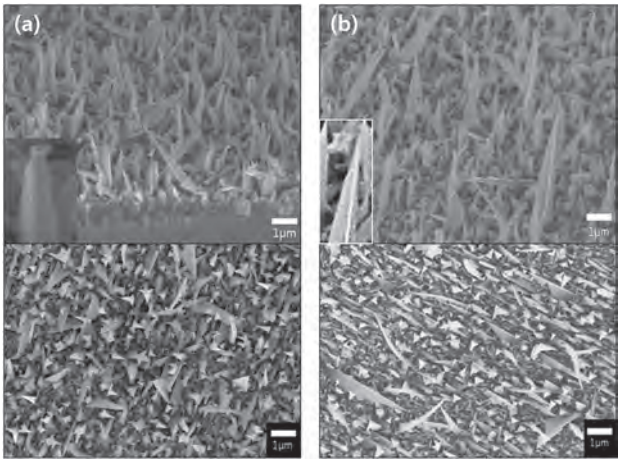

Figure 1. SEM images of the InGaN NWs grown via MOCVD at (a) 720 and (b) 730 °C. The upper panels show a tilted view, while the lower panels show a plane view. The insets in the upper panels are magnified SEM images of the tips of the InGaN NWs.

shows that no metal particles are present at the tips of the NWs, which is indicative of the change from the VLS growth mechanism to the vapor-solid-solid (VSS) growth mechanism.[10] Therefore, because of the radial growth during the VSS process, the NWs are larger, ranging from 300 nm to 5 μm in length, and from 100 to 800 nm in diameter.

Figure 2(a) shows the low-temperature (8 K), CW, μ-PL spectra of the InGaN NWs grown at 720 and 730 °C; the spectra were measured under fixed excitation conditions. The estimated peak PL wavelengths and line widths are 490 nm and 460 meV, respectively, for the sample grown at 720 °C, and 497 nm and 480 meV, respectively, for the sample grown at 730 °C. By using the standard bowing equation,[1] the stoichiometric In contents of the NWs grown at 720 and 730 °C were estimated to be 0.30 and 0.32, respectively. The other peak detected near 440 nm corresponds to the shallow localized-exciton states that are caused by either fluctuations in the In content or InGaN alloy disorders.[11] The integrated PL intensity of the NWs grown at 730 °C is approximately 1.7-times stronger than that of the NWs grown at 720 °C. This variation in the integrated PL intensities can result from differences in the active volume or internal quantum efficiency (IQE).

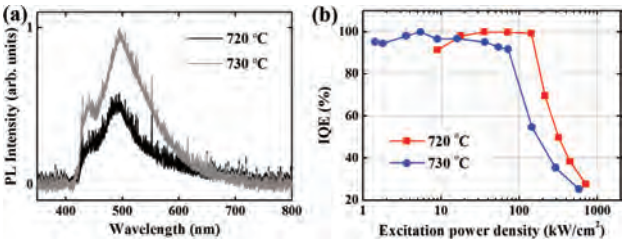

Figure 2. (a) CW μ-PL spectra of the InGaN NWs at 8 K. (b) IQE of the InGaN NWs as a function of the excitation-power density at 8 K.

To understand the difference between the IQEs of the InGaN NWs, the PL efficiency was defined as the integrated PL intensity per unit of excitation-power density under CW excitation. The IQE was defined as the ratio between the PL efficiency and the maximum PL efficiency at 8 K. In this study, it was assumed that the IQE would be approximately 100% at low temperatures because the effect of non-radiative recombination processes is negligible at such temperatures.[12] To determine the optimal excitation-power density, the excitation-power-density dependence of the IQE at low temperatures was investigated. The IQE of the InGaN NWs as a function of the excitation-power density at 8 K is plotted in Figure 2(b). The IQE of the sample grown at 720 °C is almost 100% at excitation-power densities below 140 kW/cm^2. However, the IQE rapidly decreases when the excitation-power density exceeds this threshold. This trend implies that the non-radiative recombination processes are negligible below a critical excitation-power density at low temperatures.[13] The sample grown at 730 °C also exhibits this trend, except that the critical excitation-power density is approximately 70 kW/cm^2.

Figure 3 shows the Arrhenius plots for the IQEs of the InGaN NWs. The inset graphs show the corresponding μ-PL spectra at 8 and 300 K. To avoid non-radiative recombination processes, the excitation-power density was maintained at 54 and 13 kW/cm^2 for the samples grown at 720 and 730 °C, respectively. The IQEs of the sample grown at 720 °C are almost 100%, with only small fluctuations below 150 K. However, it dramatically decreases at higher temperatures and reaches 58% at 300 K. This behavior is most likely caused by thermal quenching.[14] The sample grown at 730 °C also exhibits high IQE values of over 95% at temperatures below 120 K. However, in a similar fashion, the IQE decreases at higher temperatures and reaches 58% at 300 K. For a quantitative understanding of this thermal quenching, the experimental data was fitted with Eq. (1):

$$I = \frac{I_0}{1 + \alpha e^{-E_a/kT}} \tag{1}$$

where I_0 is the integrated PL at low temperatures, α is the process-rate parameter, and E_a is the activation energy. From the fitting results, the activation energies of the NWs grown at 720 and 730 °C were calculated to be 124 and 61 meV, respectively. This implies that the excited carriers in the NWs grown at 720 °C are more strongly confined to the localized In clusters compared to those in the NWs grown at 730 °C.

The recombination dynamics of the InGaN NWs were studied via μ-TRPL spectroscopy. Figure 4 shows the temperature-dependent PL decay times of the single-crystal InGaN NWs; fixed excitation-energy densities of 70 and 30 μJ/cm^2 were used for the samples grown at 720 and 730 °C, respectively. The insets in Figures 4(a and b) show the PL decay curves acquired at the maxima of the PL spectra of the samples at 8 and 300 K. Usually, a PL decay curve for semiconductor-based NWs cannot be represented by a simple exponential dependence because of the presence of structural disorders (e.g., nanoscale fluctuations in the In content of InGaN alloys).[11, 13] In this study, the PL decay-time constant, τ, was extracted by fitting the fast decay region with a single exponential-decay equation since the slow decay time is hard to estimate because of the low number of photons. Figure 4(a) shows that for the InGaN NWs grown at 720 °C, τ is equal to approximately 127 ps, with small fluctuations below 150 K. However, it rapidly decreases at higher temperatures, which is similar to the temperature-dependent behavior of the IQE. At 300 K, the value of τ is only 87 ps because of the increase in non-radiative recombination processes. For the InGaN NWs grown at 730 °C, τ is equal to 290 ps at 8 K, which is 2.2-times greater than that of the NWs grown at 720 °C. As the temperature increases, τ gradually decreases until 120 K is reached, and then it sharply drops beyond that threshold. To compare the obtained results with the temperature-dependent μ-PL data, the IQE values were estimated with the equations IQE $= \tau_{nr}/(\tau_{nr} + \tau_r)$ and $(1/\tau) = (1/\tau_r) + (1/\tau_{nr})$, where τ_r is the radiative decay time and τ_{nr} is the non-radiative decay time. It is assumed that τ_r is the lowest value of τ below 100 K because the non-radiative recombination processes are negligible at low temperatures.[12] Table I summarizes the estimated results, including the IQEs obtained from the integrated PL calculations. The IQE of the NWs grown at 720 °C is approximately 66%, which is slightly higher than

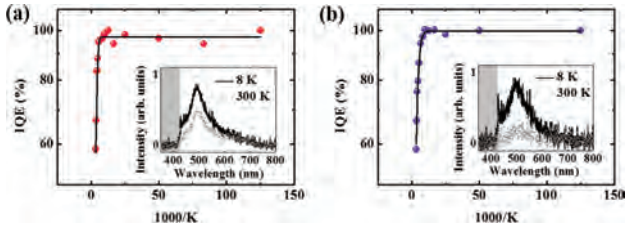

Figure 3. Temperature-dependent IQE of the InGaN NWs grown at (a) 720 and (b) 730 °C. The dots and lines indicate the measured data and fitted curves for thermal quenching.[14] The insets show the corresponding μ-PL spectra at 8 and 300 K.

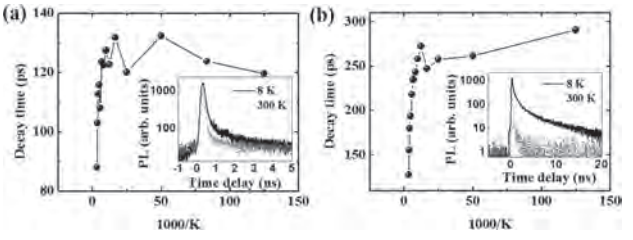

Figure 4. Temperature-dependent PL decay times of the InGaN NWs grown at (a) 720 and (b) 730 °C. The insets show the corresponding μ-TRPL curves at 8 and 300 K.

Table I. Decay-time constants and IQEs of the InGaN NWs at 300 K, which were obtained from the μ-TRPL and μ-PL spectra.

				IQE (%)	
Sample	τ (ps)	τ_r (ps)	τ_{nr} (ps)	μ-TRPL	μ-PL
Grown @ 720 °C	87	132	261	66	58
Grown @ 730 °C	127	290	228	44	58

that obtained from the temperature-dependent, integrated, μ-PL spectroscopy because of the limited time resolution of the μ-TRPL setup (approximately 100 ps). However, the IQE of the NWs grown at 730 °C is approximately 44%, which is much smaller than that obtained from the integrated μ-PL spectroscopy. This discrepancy can be attributed to the incorrect assumption that the non-radiative recombination processes caused by high excitation energies are negligible or completely frozen at low temperatures.

4. CONCLUSION

High-density InGaN NWs were synthesized via MOCVD on *r*-plane sapphire substrates at 720 and 730 °C. SEM images showed that the InGaN NWs grown at 720 °C were formed by the VLS mechanism, while the NWs grown at 730 °C were formed by sequential VLS and VSS processes. The optical properties of the single-crystal InGaN NWs were studied via μ-PL and μ-TRPL measurements under the excitation of a 403-nm laser diode. The PL intensity of the NWs grown at 730 °C was 1.7-times higher than that of the NWs grown at 720 °C. The estimated IQE of the NWs grown at 720 °C was approximately 100% below 150 K, which rapidly decreased to 58% at 300 K. However, the estimated IQE of the NWs grown at 730 °C was approximately 100% at temperatures below 100 K. The activation energy obtained by fitting the temperature-dependent IQEs of the NWs grown at 720 °C was twice that of the NWs grown at 730 °C. The PL decay times obtained from the μ-TRPL measurements for the NWs grown at 720 °C were smaller than that of the NWs grown at 730 °C at both 8 and 300 K. According to the temperature-dependent PL decay times, the IQEs of the NWs grown at 720 and 730 °C were estimated to be approximately 66% and 44%, respectively, at 300 K. These results indicate that the InGaN NWs grown at 720 °C via the VLS process are more suitable for high-efficiency light sources.

Acknowledgment: This research was supported by the National Research Foundation of Korea (NRF) grant funded by the Ministry of Science, ICT and Future Planning (MSIP) (NRF-2013R1A1A2074801).

References and Notes

1. T. Kuykendall, P. Ulrich, S. Aloni, and P. Yang, *Nature Mater.* 6, 951 (**2007**).
2. D. H. Liena, Y. H. Hsiao, S. G. Yang, M. L. Tsai, T. C. Wei, S. C. Lee, and J. H. He, *Nano Energy* 11, 104 (**2015**).
3. H. J. Xiang, S.-H. Wei, J. L. F. Da Silva, and J. Li, *Phys. Rev. B* 78, 193301 (**2008**).
4. E. Ertekin, P. A. Greaney, D. C. Chrzan, and T. D. Sands, *J. Appl. Phys.* 97, 114325 (**2005**).
5. H. C. Kuo, T. S. Oh, and P. C. Ku, *J. Cryst. Growth* 370, 311 (**2013**).
6. H.-M. Kim, H. Lee, S. I. Kim, S. R. Ryu, T. W. Kang, and K. S. Chung, *Phys. Status Solidi B* 241, 2802 (**2004**).
7. K. M. Wu, Y. Pan, and C. Liu, *Appl. Surf. Sci.* 255, 6705 (**2009**).
8. T. Tabata, J. Paek, Y. Honda, M. Yamaguchi, and H. Amano, *Phys. Status Solidi C* 9, 3 (**2012**).
9. G. T. Wang, A. A. Talin, D. J. Werder, J. R. Creighton, E. Lai, R. J. Anderson, and I. Arslan, *Nanotechnology* 17, 5773 (**2006**).
10. W. Lu and J. Xiang, Semiconductor Nanowires: From Next-Generation Electronics to Sustainable Energy, Royal Society of Chemistry, Cambridge (**2014**).
11. G. You, W. Guo, C. Zhang, P. Bhattacharya, R. Henderson, and J. Xu, *Appl. Phys. Lett.* 102, 091105 (**2013**).
12. S. Watanabe, N. Yamada, M. Nagashima, Y. Ueki, C. Sasaki, Y. Yamada, T. Taguchi, K. Tadatomo, H. Okagawa, and H. Kudo, *Appl. Phys. Lett.* 83, 4906 (**2003**).
13. H. Murotani, Y. Yamada, T. Tabata, Y. Honda, M. Yamaguchi, and H. Amano, *J. Appl. Phys.* 114, 153506 (**2013**).
14. J. Krustok, H. Collan, and K. Hjelt, *J. Appl. Phys.* 81, 1442 (**1997**).

Received: 24 November 2015. Accepted: 29 June 2016.